



## Too hot to handle? On the cooling capacity of urban green spaces in a Neotropical Mexican city



Richard Lemoine-Rodríguez <sup>a,b,c</sup>, Luis Inostroza <sup>a,d,e</sup>, Ina Falfán <sup>f,g</sup>, Ian MacGregor-Fors <sup>h,\*</sup>

<sup>a</sup> Institute of Geography, Ruhr-Universität Bochum, Universitätsstr. 150, 44780 Bochum, Germany

<sup>b</sup> Geolinguist Studies Team, University of Würzburg, Am Hubland 97074, Würzburg, Germany

<sup>c</sup> Earth Observation Center, German Aerospace Center, Oberpfaffenhofen 82234, Germany

<sup>d</sup> Faculty of Regional Development and International Studies, Mendel University in Brno, Zemědělská 1/1665, 613 00 Brno, Czech Republic

<sup>e</sup> Universidad Autónoma de Chile, 7500912 Santiago, Chile

<sup>f</sup> Red de Ambiente y Sustentabilidad, Instituto de Ecología, A.C., Carretera antigua a Coatepec 351, El Haya, Xalapa, 91073 Veracruz, Mexico

<sup>g</sup> Laboratorio de Restauración Ecológica, Instituto de Biología, Universidad Nacional Autónoma de México, Circuito Exterior, 04510, Coyoacán, Ciudad de México, Mexico

<sup>h</sup> Faculty of Biological and Environmental Sciences, University of Helsinki, Niemenkatu 73, FI-15140 Lahti, Finland

### ARTICLE INFO

#### Keywords:

Cooling range  
Green infrastructure  
Heat mitigation  
SUHI  
Urban climate  
Urban planning

### ABSTRACT

Urban areas are particularly vulnerable to climate change due to the Urban Heat Island (UHI) effect, which can be mitigated by urban vegetation through shading and evapotranspiration. Nevertheless, there is still a lack of spatially explicit information on the cooling capacity of green infrastructure for most Latin American cities. In this study, we employed Land Surface Temperature (LST) of the Neotropical Mexican city of Xalapa to (1) analyze its Surface UHI (SUHI) compared to its peri and extra-urban areas, (2) to assess the cooling capacity of urban green spaces larger than 1 ha, and (3) to evaluate the role of green spaces' size, shape and their surrounding tree cover percentage (Tc) on green spaces cooling range. We evaluated the cooling range of green spaces and their relationships with green spaces metrics and Tc via a linear mixed-effect model and identified threshold values for the variables at 25 m, 50 m, 100 m, and 200 m from the borders of green spaces through Classification and Regression Trees. Xalapa exhibits a SUHI of 1.70 °C compared to its peri-urban area and 4.95 °C to the extra-urban area. Green spaces > 2 ha mitigated heat at ~2 °C and the cooling range was influenced by the size of green spaces ≥ 2.8 ha and Tc > 21% at 50 m and only by Tc surrounding the green spaces at 100 m and 200 m. This shows that the size threshold of urban green spaces should be complemented with the presence of Tc starting at least 50 m to maximize the cooling capacity provided by the green infrastructure. Planning agendas should account for the interaction between the size of green spaces and the cumulative cooling effect of scattered vegetation inside urban areas towards compact green cities to cope with urban warming.

### 1. Introduction

Due to the thermal properties of their material components, urban areas exhibit the so-called urban heat island (UHI) effect, which provides the most dramatic evidence of human activities' impact on local climate (Peng et al., 2012; Yang et al., 2016). The UHI term refers to the fact that urban areas are generally warmer than their surroundings (Oke, 1995). Currently, it is one of the most documented phenomena of local

climate change (Santamouris, 2015).

The UHI was first assessed using air temperatures, measured by in-situ weather stations, to analyze the urban canopy layer, which extends from the ground to the building's rooftops and represents the area on which urban inhabitants experience local temperatures (Oke et al., 2017). In the last decade, an increasing body of literature has focused on the surface UHI (SUHI) assessment, due to the increasing availability of remote sensing data, which enabled the analysis of spatially continuous

\* Correspondence to: Ecosystems and Environment Research Programme, Faculty of Biological and Environmental Sciences, University of Helsinki, Niemenkatu 73, FI-15140 Lahti, Finland.

E-mail addresses: [richard.lemoine-rodriguez@uni-wuerzburg.de](mailto:richard.lemoine-rodriguez@uni-wuerzburg.de) (R. Lemoine-Rodríguez), [Luis.Inostroza@rub.de](mailto:Luis.Inostroza@rub.de) (L. Inostroza), [isfalfan@yahoo.com.mx](mailto:isfalfan@yahoo.com.mx) (I. Falfán), [ian.macgregor@helsinki.fi](mailto:ian.macgregor@helsinki.fi) (I. MacGregor-Fors).

urban land surface temperature (LST) information, based on systematically acquired satellite images (Chakraborty and Lee, 2019; Clinton and Gong, 2013; Peng et al., 2012). LST modulates the lower layer of urban air temperatures and affects energy fluxes, influencing human comfort (Voogt and Oke, 2003). Although UHI and SUHI are not equal, empirical evidence shows that both are coupled and correlated (Nichol et al., 2009; Prihodko and Goward, 1997). Therefore, relevant insights for urban planning can be derived from the LST and SUHI indicators.

SUHIs cause several negative consequences for urban inhabitants; thus becoming one of the main urban planning challenges of the twenty-first century (Rizwan et al., 2008; Yow, 2007). SUHIs promote heat stress especially in the warmest season, affecting human well-being by increasing (i) cooling energy and water use and its associated costs, (ii) air pollution, (iii) thermal discomfort, (iv) spread of vector-borne diseases, and (v) heat-related health incidences (Heisler and Brazel, 2010; Mohajerani et al., 2017; Nuruzzaman, 2015). It has been shown that the SUHI effect and heat waves are synergistic, with SUHI causing increased heat wave frequencies and heat waves intensifying the SUHI effect, increasing heat-related mortality in urban areas (Tan et al., 2010; Zhao et al., 2018).

Diverse strategies to mitigate the SUHI effect have been proposed, such as planning and management of street geometry (e.g., built-up distribution and density, design, height, and orientation) and vegetation cover (e.g., ground vegetation, shade trees, urban parks, green roofs, green walls and facades). Other climate adaptation strategies include the use of cool materials with high albedo for buildings and pavements (e.g., reflective coatings, smother surfaces), and incorporation of waterbodies and water-retaining pavements. Each mitigation strategy causes different effects on radiation, wind path, wind speed, temperature, humidity, and thermal comfort (Akbari and Kolokotsa, 2016; Lai et al., 2019; Nuruzzaman, 2015; Rizwan et al., 2008; Xu et al., 2019, 2017). Nonetheless, the most studied and applied strategies for SUHI mitigation involve vegetation cover due to its potential and possible implementation through urban planning at the city scale (Aleksandrowicz et al., 2017; Aram et al., 2019a, 2019b; Duncan et al., 2019).

The use of green infrastructure to mitigate SUHIs includes implementing green roofs, green facades, greenways, urban forests, parks, and other green spaces (Aram et al., 2019a; Bowler et al., 2010), which help to mitigate diurnal SUHIs by modulating temperature through shading and evaporative cooling (Chakraborty and Lee, 2019; Clinton and Gong, 2013; Higueras, 2006; Peng et al., 2012). Due to these properties, urban green spaces are generally cooler than their impervious surrounding areas (Chibuike et al., 2018; Lin et al., 2015; Yan et al., 2018). The cooling capacity of green infrastructure can be extended several meters beyond its boundaries (i.e., the cooling range). Nonetheless, cooling capacity varies according to the plant type, canopy density, connectivity, shape, and size of vegetation patches across urban areas (Aram et al., 2019a; Chen et al., 2014; Xiao et al., 2018).

Due to the multiple factors influencing SUHIs across different climatic backgrounds, each SUHI exhibits specific dynamics (Lemoine-Rodríguez et al., 2022; Yow, 2007). Knowledge on SUHIs and the cooling capacity of local urban green spaces is essential to implement heat mitigation strategies in urban areas (Du et al., 2017; Norton et al., 2015; Yu et al., 2017). Woefully, SUHI research has been mainly focused on the temperate regions of Europe, North America, and Asia, and, to a lesser extent, on African and Latin American cities (Chakraborty et al., 2020; Liu et al., 2021; Schwarz and Manceur, 2015). For African and Latin American subtropical and tropical regions, knowledge about SUHI dynamics and their possible mitigation strategies, including the use of urban green spaces, is still underrepresented in the urban climate and urban planning literature (Aleksandrowicz et al., 2017; Aram et al., 2019a; Bowler et al., 2010; Roth, 2007). Nonetheless, cities showing intense SUHIs (i.e.,  $\geq 3^{\circ}\text{C}$  annual average during daytime) are distributed in these regions (Peng et al., 2012). Analyses of Latin American cities' SUHIs are particularly relevant because this region has a high

percentage of urban population (81 %), mainly distributed in medium-sized and small cities (United Nations, 2019). Therefore, the largest amount of population experiencing the negative health impacts of the SUHI effect are located in these types of cities. Knowledge of heat mitigation strategies to inform planning is crucial for Latin American cities since they have shown high levels of social heat vulnerability and lack of adaptive capacity (Huang et al., 2019; Inostroza et al., 2016). Projected scenarios suggest that cities in this region, particularly the ones located in tropical areas, will suffer the highest levels of warming due to urbanization in the coming years (Huang et al., 2019). Moreover, medium-sized cities are expanding at the fastest pace and they are the most dynamic areas in terms of urban form change (Lemoine-Rodríguez et al., 2020). Most of these cities lack spatially explicit information on their corresponding SUHIs and the cooling capacity of their green infrastructure to mitigate high temperatures (Palme, 2021).

Empirical evidence shows that patch size is the main variable influencing the internal LST of urban green spaces (Du et al., 2017; Liang et al., 2020; Yu et al., 2017). Additionally, high tree cover and simple overall patch shape (i.e., round) promote lower LST inside urban parks (Wang et al., 2021; Yu et al., 2017). The spatial arrangement and composition of vegetation patches also influence the cooling range of urban parks, showing a negative correlation between green spaces' size and simple shape and the LST in surrounding areas (Chen et al., 2014; Huang et al., 2018; Yu et al., 2017). Here, scattered vegetation patches surrounding urban parks can also contribute to reduce LST (Chen et al., 2014; Geng et al., 2022; He et al., 2021). Nevertheless, it is not yet clear what is the cumulative cooling effect of urban parks and their surrounding tree cover across the urban tissue.

Aiming to contribute with spatially explicit information for the management and planning of Latin American cities, in this study we assess the SUHI intensity and cooling capacity of the green spaces of Xalapa, Veracruz, Mexico at different spatial units. While it is well-known that urban green spaces have the potential to mitigate SUHI, the cumulative cooling contribution of urban parks and surrounding smaller green patches is not yet clear. Our objectives were: (1) to analyze the SUHI along the gradient of urbanization of the city (2) to assess the effect of the shape and size of the green spaces on their internal LST, and (3) to evaluate the interplay between the green spaces' shape and size and surrounding tree cover (Tc) on their cooling range across the city at different distances. Our main research questions were: (1) is there a cumulative cooling effect between urban parks and smaller surrounding green spaces inside the city? (2) which variables are relevant for cooling at different distances from the green patches' borders (i.e., shape, size or surrounding Tc), and (3) in which way do these variables interact across space inside the city? The main contribution of this research is the quantitative relationship between the size and shape of urban green spaces, as well as the contribution of scattered vegetation (mixed land use) across the urban tissue to mitigate urban heat in a Neotropical medium-sized Latin American city. Moreover, the spatial interaction between these variables was assessed to measure the cumulative cooling effect of the green infrastructure at different distances. This assessment provides relevant insights for planning green infrastructure maximizing its cooling capacity and cooling range inside the city, based on empirical evidence.

## 2. Methods

### 2.1. Study area

We conducted this study in the city of Xalapa, a medium-sized Neotropical city located in Eastern Mexico ( $19^{\circ}32'50''$  North,  $96^{\circ}55'10''$  West; Fig. 1). The city is the state capital of Veracruz and covers an area of  $65.5 \text{ km}^2$ , with a population of  $\sim 550\,000$  inhabitants (INEGI, 2021; Lemoine-Rodríguez et al., 2019). Due to its elevation range (600 masl: 1120–1720 masl), Xalapa has subtropical highland (Cfb; Northwest) and humid subtropical (Cfa; Southeast) climates, with

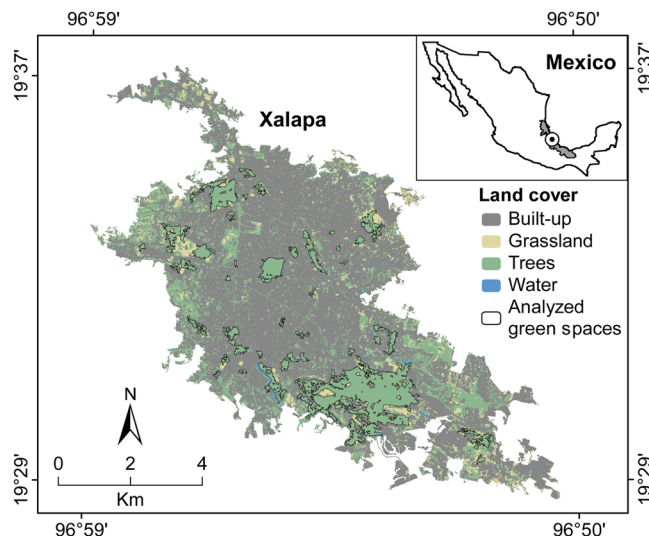


**Fig. 1.** Location and land cover map of Xalapa highlighting the urban green spaces assessed in this study.

an annual mean precipitation of 1493 mm (Kottek et al., 2006). The annual mean temperature is 18 °C, ranging between 7 °C in winter to 35 °C in summer, with the highest temperatures in April and May (INEGI, 2014; Soto-Esparza and Gómez-Columna, 1993). The original vegetation covering the region before the city development, predominantly consisted of cloud forest (Rzedowski, 1978), followed by tropical dry forest and riparian vegetation (Castillo-Campos, 1991). Preexisting urban green cover decreased as a consequence of infill urbanization in Xalapa, while new green patches were embedded in the city as it expanded, leading to the current woody vegetation cover of ~20% inside the city (Lemoine-Rodríguez et al., 2019). Urban vegetation in Xalapa is mainly distributed in private gardens, public parks, ecological parks, median strips, and forest patches, composed by a significant number of exotic plant species (Capitanachi et al., 2004; Falfán and MacGregor-Fors, 2016).

## 2.2. Land surface temperature retrieval

To compute the LST of Xalapa, we employed a Landsat 8 OLI/TIR image from April 12th of 2019, the warmest month of the year for which a high-quality image was available, with a 30 m spatial resolution and no cloud cover on the city area. We preprocessed the image by applying a Dark Object Subtraction (DOS) image-based atmospheric correction to the visible and infrared bands in order to obtain surface reflectance values (Chavez, 1996), using the RStoolbox R package (Leutner et al., 2019). All further processing steps were conducted in R (R Core Team, 2019), by means of the R-package LSTtools (Lemoine-Rodríguez and Mas, 2020) to process thermal data. We converted the Digital Numbers (DN) contained in the Thermal Infrared band 10 (TIR) to at sensor spectral radiance ( $L_\lambda$ ), employing the multiplicative and rescaling factors contained in the image metadata, as suggested by USGS (2019; Eq. 1).

$$L_\lambda = ML * Q_{cal} + AL \quad (1)$$

Where:

$ML$ = Radiance multiplicative scaling factor of the band.

$Q_{cal}$ = Pixel value in DN.

$AL$ = Radiance additive scaling factor of the band.

To compute LST, it was necessary to estimate the ground emissivity values for each pixel in the image, for which we applied the modified Normalized Difference Vegetation Index (NDVI) threshold method

(Sobrino et al., 2008). We computed the NDVI employing the Red and Near Infrared (NIR) bands. Based on the NDVI values, the modified NDVI threshold method classifies pixels into soil pixels ( $NDVI_S < 0.2$ ), fully vegetated pixels ( $NDVI_V > 0.5$ ) and mixed pixels (i.e., pixels with mixed infrastructure and vegetation, none of them showing a pixel proportion of  $> 0.8$ ;  $NDVI \geq 0.2$  and  $NDVI \leq 0.5$ ). According to this, fixed emissivity values of 0.97 for soil pixels and 0.99 for vegetated pixels were defined. For mixed pixels, emissivity was computed following Eq. (2):

$$\varepsilon = \varepsilon_S + (\varepsilon_V - \varepsilon_S) * P_V \quad (2)$$

where:

$\varepsilon_S$ = Soil emissivity.

$\varepsilon_V$ = Vegetation emissivity.

$P_V$ = Proportion of vegetation, computed based on the NDVI as follows (Eq. 3):

$$P_V = \left( \frac{NDVI - NDVI_S}{NDVI_V - NDVI_S} \right)^2 \quad (3)$$

We derived the brightness temperature (BT) from the at sensor radiance of the TIR band (Eq. 4). After this, we corrected the BT values using the Planck function, adding the influence of the computed per-pixel emissivity and then converting the values from Kelvin to Celsius degrees (Eq. 5).

$$BT = \frac{K_2}{\ln\left(\frac{K_1}{L_\lambda}\right)} + 1 \quad (4)$$

where:

$L_\lambda$ = At sensor radiance ( $W/(m^2 * sr * \mu\text{m})$ ).

$K_1$ = Calibration constant ( $W/(m^2 * sr * \mu\text{m})$ ).

$K_2$ = Calibration constant (K)

$$LST = \frac{BT}{1 + \left(\frac{\lambda * BT}{\rho}\right) * \ln(\varepsilon)} - 273.15 \quad (5)$$

where:

$BT$ = Brightness temperature.

$\lambda$ = Central band wavelength of emitted radiance.

$\rho = h * c / \sigma$  ( $1.438 * 10^{-2} \text{ m}^3 \text{ K}$ ), where  $\sigma$  is the Boltzmann constant ( $1.38 * 10^{-23} \text{ J/K}$ ),  $h$  is the Planck's constant ( $6.626 * 10^{-34} \text{ J*s}$ ), and  $c$  is the light velocity ( $2.998 * 10^8 \text{ m/s}$ ).

$\varepsilon$ = Emissivity.

## 2.3. Surface urban heat island assessment

To assess the urban temperatures of Xalapa, we employed the SUHI intensity indicator, which measures the difference between LST inside the city and its surroundings (Oke, 1973). We computed the SUHI intensity based on the mean LST at three spatial units representing the gradient of urbanization: (i) the urban area (represented by the dense continuous built-up), (ii) the peri-urban area (delineated as an inner buffer of 420.51 m from a smoothed limit of the city polygon according to MacGregor-Fors (2010), and (iii) the extra-urban area (defined by an outside buffer from the smoothed city polygon at the same distance than the peri-urban area; Fig. 2). To spatially define the urban green spaces, we employed land cover data including 'built-up', 'grassland', 'water' and 'trees' (Lemoine-Rodríguez et al., 2019). This cartography was based on a SPOT image with a spatial resolution of 2.5 m and achieved an overall map accuracy  $> 82\%$ . Finally, we computed the proportion of vegetation ('trees' and 'grassland' land cover classes) for the urban, peri-urban, and extra-urban areas.

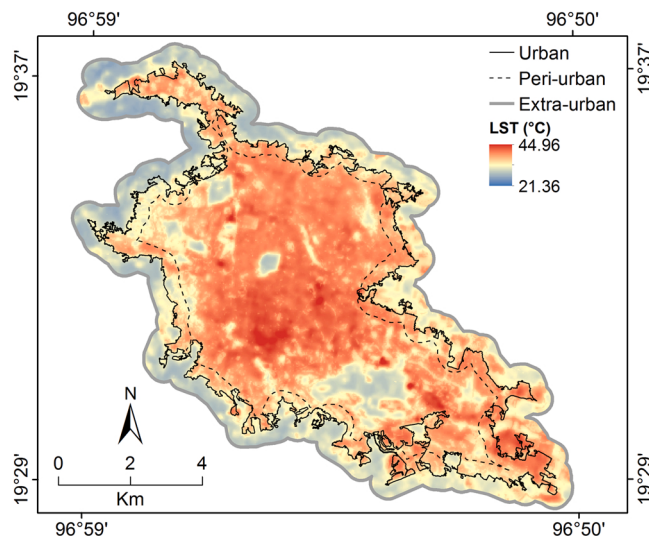


**Fig. 2.** LST values in Xalapa for the spatial units representing the urbanization gradient of the city.

#### 2.4. Green space delineation and computation of landscape metrics

For the delineation of green spaces, we extracted and updated the class ‘trees’ from the land cover classification, based on the 2019 Landsat image (Fig. 3). We did not consider the administrative boundaries of the green spaces (e.g., official urban parks), but the continuous

tree cover, since official limits do not accurately represent the extension of the vegetation for most tree cover patches.

To assess if a relationship exists between the size and shape of the green spaces and their LST and cooling capacity, we computed the Patch Area (PA) and the Shape Index (SI) landscape metrics at patch level, following McGarigal et al. (2012; Fig. 3). PA is measured in hectares and is a metric that reflects the size of the patch. SI reflects configuration and is considered the most straightforward measure of overall shape complexity. When a patch is compact (i.e., square or circle), SI is equal to one and increases without limit as patch shape becomes more irregular (McGarigal et al., 2012).

#### 2.5. Relationship between cooling capacity and landscape metrics

We employed a linear regression model (LM; multiplicative) to test for relationships between the internal LST of the green spaces and their spatial metrics (i.e., PA and SI in their log forms due to skewed distributions given by the largest green area of the city; Fig. 3). To assess the extent of the cooling range provided by the urban green spaces (i.e., the distance from the green spaces’ borders up to which they provide a cooling effect) in a spatially explicit manner, we defined a set of external spatial buffers at 25 m, 50 m, 100 m, and 200 m from the border of tree cover patches in the city > 1 ha ( $n = 40$ ; Figs. 1, 3 and 4a). The selection of distances was based on the scale of analysis and the aim of representing intraurban LST differences across the city. Our maximum distance (200 m) was defined to avoid high overlap between buffers and surrounding green spaces. We assessed the cooling capacity-distance relationship (i.e., cooling range) by comparing the mean LST of green spaces with that of each buffer distance employing a linear mixed-effect

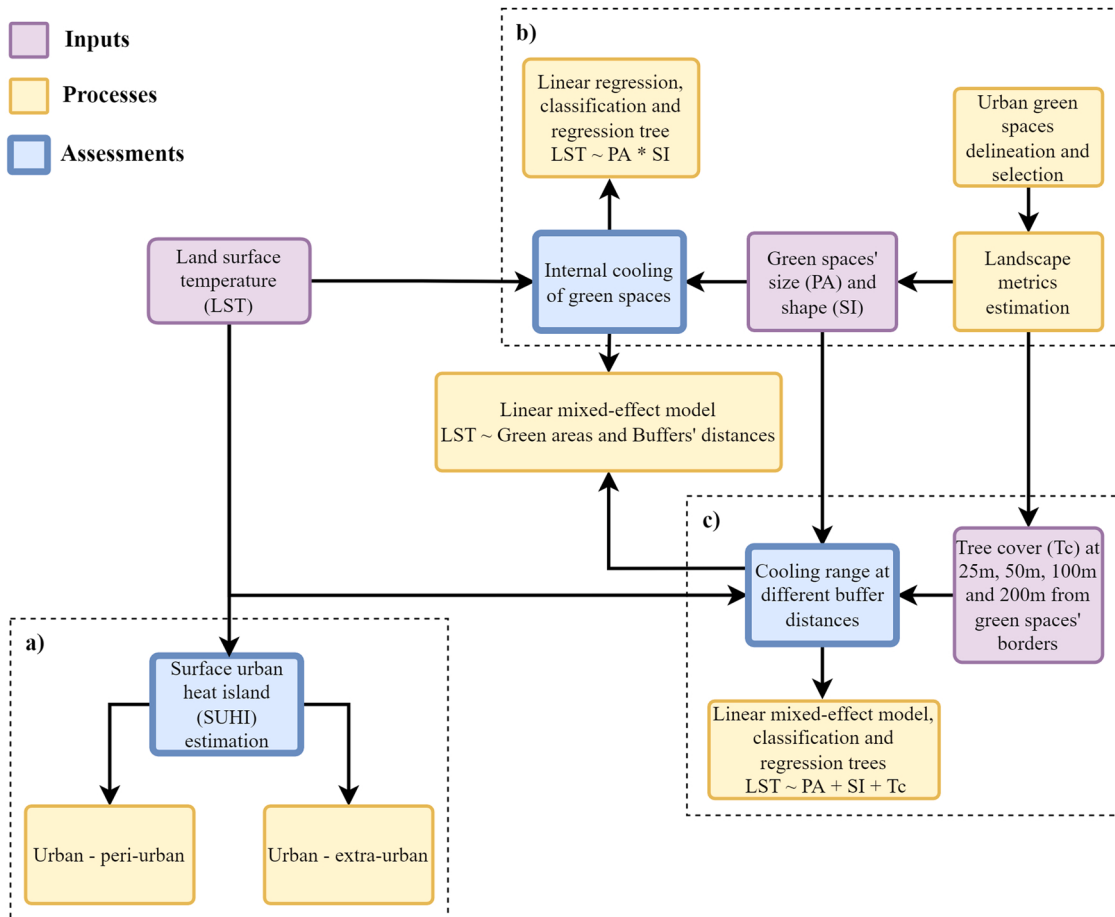


**Fig. 3.** Steps carried out to conduct the a) SUHI, b) green spaces’ internal cooling capacity, and c) green spaces’ cooling range assessments. Arrows indicate the work flow and dashed squares correspond to each assessment.

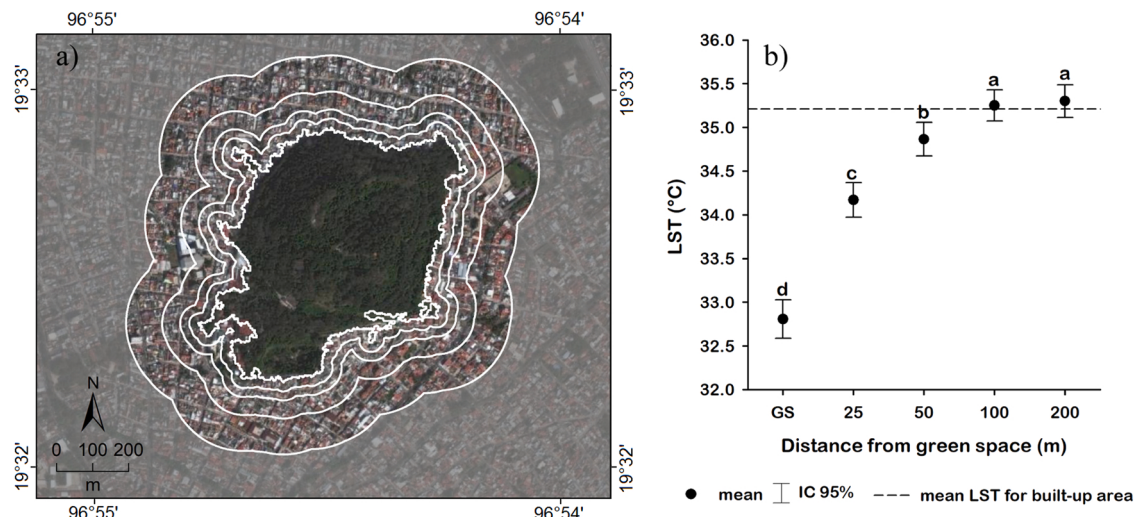


**Fig. 4.** a) Example of buffers for an urban green area at 25 m, 50 m, 100 m, and 200 m and b) green spaces (GS) cooling capacity-distance plot (cooling range) showing results of Tukey contrasts.

model (LMM, Pinheiro et al., 2020). We computed subsequent Tukey contrasts from this model to identify pairwise differences in LST of green spaces and the consecutive buffers (Lenth et al., 2020). For the case of LST at each buffer distance from the green spaces' borders, we assessed the same spatial metrics plus the tree cover percentage (Tc) inside buffers using a LMM to test the green spaces' cooling range (Fig. 3). Finally, to identify thresholds for LST inside the green spaces and buffers concerning PA and SI metrics and Tc in the buffers, we carried out Classification and Regression Trees (CARTs; Fig. 3; Therneau and Atkinson, 2018; as suggested by Bowler et al., 2010).

### 3. Results

#### 3.1. Urban heat island of Xalapa

The LST values of Xalapa exhibit a clear gradient related to the degree of urbanization of each spatial unit (Fig. 2; Table 1). Lowest values of LST are mainly distributed in the surroundings of the urban fringe (North and West), where forest patches are located, and along the larger urban green spaces of the city polygon (Fig. 2). Intermediate values of LST are located in the South and East of the city, where grassland patches are distributed. The urbanized area of the city exhibited the lowest proportion of vegetation and the highest mean LST. Mean LST decreases while proportion of vegetation increased in the peri-urban and extra-urban areas of the city. Xalapa exhibited a mean SUHI effect with an intensity of 1.70 °C compared to the peri-urban area and 4.95 °C based on the extra-urban area. The highest standard deviation was present inside the urban polygon, followed by the extra-urban and peri-urban areas (Table 1).

#### 3.2. Effect of configuration and composition on green spaces' land surface temperature

LST of the analyzed green spaces > 1 ha in Xalapa ranged from 26.68 °C to 38.81 °C with a mean value of 30.46 °C ( $\pm 2.26$  °C SD). The PA of these spaces varied from 1.01 ha to a maximum of 326.13 ha, with

a mean value of 15.48 ha ( $\pm 50.64$  ha SD) and the SI ranged from 2.16 to 9.90, with a mean of 3.87 ( $\pm 1.53$  SD), indicating mainly an irregular form for the green spaces (Fig. 1). The LM results showed a negative and significant association of green spaces' LST with PA variation ( $F_{1,37} = 49.50$ ,  $p < 0.001$ ), and a negative non-significant tendency with SI ( $F_{1,37} = 1.02$ ,  $p = 0.319$ ). On the other hand, the interaction between PA and SI showed a non-significant trend ( $F_{1,37} = 3.49$ ,  $p = 0.070$ ). Accordingly, green spaces with the lowest mean LST were mainly the largest ones: 'Cerro de Macuitlapetl' (29.09 °C, 31.32 ha), 'Cerro de la Galaxia' (29.23 °C, 48.50 ha), 'Lomas del Seminario' (29.43 °C, 20.34 ha) and 'Parque Natura' (29.66 °C, 326.13 ha). The results from the corresponding CART (Fig. 5), pointed to green spaces  $\geq 6.4$  ha as cooler by 3 °C on average than those  $< 6.4$  ha. Green spaces  $< 2$  ha had warmer LST by 4 °C on average, compared to green spaces  $\geq 6.4$  ha.

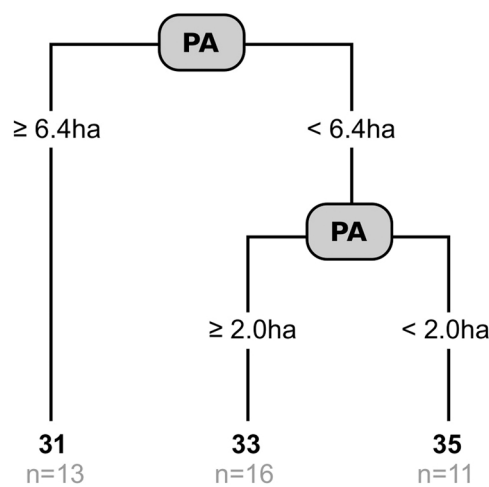


**Fig. 5.** Classification and regression tree (CART) showing the relationships between LST and green spaces' metrics.

**Table 1**

Descriptive statistics of urban, peri-urban and extra-urban LST (°C), SUHI (°C), and proportion of vegetation.

Spatial unit	Min.	Max.	Range	Mean	SD	SUHI intensity (peri-urban, extra-urban)	Proportion of vegetation
Urban	26.68	41.20	14.52	34.12	2.53	1.70, 4.95	20.35
Peri-urban	25.03	38.72	13.69	32.42	2.35	–	36.21
Extra-urban	24.71	38.38	13.67	29.17	2.40	–	85.06

### 3.3. Effect of configuration and composition on cooling range

The LMM results indicated that LST increased with larger distance from the green spaces ( $F_{4,156.01} = 142.46$ ,  $p < 0.001$ ; **Table 2**). According to Tukey contrasts, LST of green spaces was significantly lower than LST of buffers and LST differed significantly between consecutive buffers, except between 100 m and 200 m (**Table 3**, **Fig. 4b**). Therefore, the cooling range of green spaces in Xalapa extends up to 50 m from their borders. According to the second LMM, LST at the four evaluated buffer distances showed negative linear relationships with PA ( $F_{1,38} = 10.04$ ,  $p = 0.003$ ) and Tc ( $F_{1,118} = 30.48$ ,  $p < 0.0001$ ). Namely, smaller green spaces and lower tree cover percentages derive in higher LST as distance increases from the borders of the green spaces (**Figs. 6 and 7**). CARTs corroborated the LMM results and showed differential relevance of PA and Tc at each buffer distance. Specifically, PA was the only relevant variable affecting buffers' LST at 25 m and was an important variable at 50 m, but it was not relevant at 100 m and 200 m. Furthermore, PA  $\geq 6.4$  ha exhibited the highest cooling effect at 25 m and PA  $< 2.8$  ha showed no cooling effect. On the other hand, Tc interacted with PA to influence the cooling range at 50 m, mainly when Tc was  $< 21\%$  and green spaces size was  $\geq 2.8$  ha. With values  $\geq 21\%$  at 50 m,  $\geq 18\%$  at 100 m, and  $\geq 22\%$  at 200 m, Tc was the only relevant factor for LST regulation inside the buffers (**Fig. 8**).

## 4. Discussion

### 4.1. Surface urban heat island of Xalapa

Like most cities located in non-arid climates, the city of Xalapa exhibits a positive diurnal SUHI ([Chakraborty and Lee, 2019](#); [Clinton and Gong, 2013](#); [Lemoine-Rodríguez et al., 2022](#)). This effect has already been reported for the city, albeit following different, mainly non-spatially continuous methodological approaches ([Barradas, 1987](#); [Méndez Romero, 2017](#); [Tejeda-Martínez and Acevedo-Rosas, 1990](#)). Our work is the first spatially explicit and continuous SUHI assessment of Xalapa, which employs a clear delineation of the assessed spatial units. The SUHI of Xalapa compared to its extra-urban area ( $4.95^{\circ}\text{C}$ ) is within the intensity range of other Latin American areas (i.e.,  $3\text{--}8^{\circ}\text{C}$ ), such as Mexico City, Santiago de Chile, Sao Paulo, Rio de Janeiro, and Belo Horizonte ([Lemoine-Rodríguez et al., 2022](#); [Montaner-Fernández et al., 2020](#); [Monteiro et al., 2021](#); [Sarricolea and Meseguer-Ruiz, 2019](#)). Compared to other Mexican cities, the SUHI of Xalapa is higher than larger cities such as Guadalajara and Monterrey ([Roth, 2007](#)). Yet, our results differ from the previously reported maximum UHI intensity of  $7^{\circ}\text{C}$  for the city ([Tejeda-Martínez and Acevedo-Rosas, 1990](#)). Here, it is important to consider that those authors compared the temperature of downtown Xalapa with that of Las Vigas, Veracruz as the external reference. Las Vigas is located  $\sim 35$  km northwest from Xalapa, at  $\sim 2400$  masl, and with a subhumid moderate rainy summer ([Pereyra Díaz et al., 1992](#)). Furthermore, [Tejeda-Martínez and Acevedo-Rosas \(1990\)](#) argue that the "not extremely intense" UHI effect of  $7^{\circ}\text{C}$  was due to the few industries and to the high vegetation density in and around Xalapa. It has been shown that cities with fragmented spatial patterns as consequence of sprawled urban development (i.e., low-dense and dispersed urbanization) exhibit strong SUHI intensity due to high

**Table 2**

Descriptive statistics of LST ( $^{\circ}\text{C}$ ) for green spaces and buffers.

Spatial unit	Min.	Max.	Mean	SD	$\Delta$ mean LST - preceding spatial unit
Green spaces	26.68	38.81	30.46	2.26	–
25 m	27.72	39.69	33.20	2.02	2.74
50 m	28.33	40.69	34.23	1.96	1.03
100 m	27.34	41.20	34.63	2.08	0.40
200 m	27.15	41.04	34.89	2.20	0.26

**Table 3**

Tukey contrasts for green spaces and buffers.

Contrast	Estimate	SE	Df	t ratio	p
GS - 25 m	-1.36	0.123	156	-11.09	< 0.0001
GS - 50 m	-2.06	0.123	156	-16.74	< 0.0001
GS - 100 m	-2.44	0.123	156	-19.87	< 0.0001
GS - 200 m	-2.49	0.123	156	-20.27	< 0.0001
25–50 m	-0.70	0.123	156	-5.65	< 0.0001
25–100 m	-1.08	0.123	156	-8.78	< 0.0001
25–200 m	-1.13	0.123	156	-9.18	< 0.0001
50–100 m	-0.39	0.123	156	-3.13	0.018
50–200 m	-0.43	0.123	156	-3.53	0.005
100–200 m	-0.05	0.123	156	-0.40	0.994

tree cover loss ([Lu et al., 2020](#); [Stone et al., 2010](#)). Xalapa has exhibited an increasingly sprawled urban expansion in the latest decades, adding forest patches from its periphery while reducing pre-existent urban green spaces due to infill urbanization ([Lemoine-Rodríguez et al., 2019](#)). Despite Xalapa lacks proper city planning,  $\sim 20\%$  of the city area corresponds to Tc ([Lemoine-Rodríguez et al., 2019](#)), with positive effects on SUHI mitigation. While it is necessary to promote a less sprawled urban development, the preservation of an urban interconnected green infrastructure with the aim of strengthening its mitigation effects on SUHI and climate change will be challenging, especially considering the low contribution of small green areas to heat mitigation.

Several cities exhibiting intense SUHIs (i.e.,  $\geq 3^{\circ}\text{C}$  annual daytime mean) are distributed in Latin American tropical and subtropical areas (e.g., Sao Paulo, Bogota, Mexico City; [Peng et al., 2012](#)). Nevertheless, comparisons with other settlements of similar size and climate are limited due to the lack of information for medium-sized Latin American cities and different methods employed to compute SUHI ([Inostroza, 2014](#); [Montaner-Fernández et al., 2020](#); [Monteiro et al., 2021](#)). Moreover, the lack of standardization in the assessment of SUHI and LST, such as the delineation of the urban area and external reference, adds high uncertainty to cross-city comparisons ([Lemoine-Rodríguez et al., 2022](#)).

The assessment of the thermal urban environment should not only be based on the SUHI indicator, since this metric is context-dependent (i.e., influenced by elevation, local climate, delineation of spatial units) and does not represent the temperatures that urban inhabitants experience ([Lemoine-Rodríguez et al., 2022](#)). LST and air temperatures need to be considered in the assessments in order to compare surface and canopy urban temperatures with local heat stress thresholds and therefore to determine if temperatures are actually a health risk for the population ([Martilli et al., 2020](#)).

### 4.2. Urban green spaces' structure and cooling capacity

The relevance of green spaces to mitigate the SUHI effect has been proven at global ([Clinton and Gong, 2013](#); [Peng et al., 2012](#); [Yang et al., 2021](#)) and local scales ([Kong et al., 2014](#); [Li et al., 2012](#); [Wang et al., 2021](#); [Yu et al., 2017](#)). Since daytime LST is particularly high in tropical and temperate cities ([Yang et al., 2021](#)), recently, there has been an increasing interest in the study of urban temperatures in such climates.

The relationship between the spatial structure of urban green spaces and LST is complex and influenced by several factors. We analyzed the cooling capacity of green spaces during the warmest month, since the strongest cooling effect from vegetation is provided during this time of the year ([Chen et al., 2014](#); [Duncan et al., 2019](#); [Huang et al., 2018](#)). In line with our findings, green patch size has been proven to have the strongest influence on the LST inside green spaces, as well as on their cooling range ([Du et al., 2017](#); [Liang et al., 2020](#); [Yu et al., 2017](#)). This is the result of the cumulative evaporative cooling, lower thermal inertia and shading provided by larger vegetated areas ([Weng et al., 2004](#)). While this relationship is already known, detailed studies show that the effect of patch size is context-dependent and should be analyzed at local scales. In fact, the same vegetation structure in different locations will

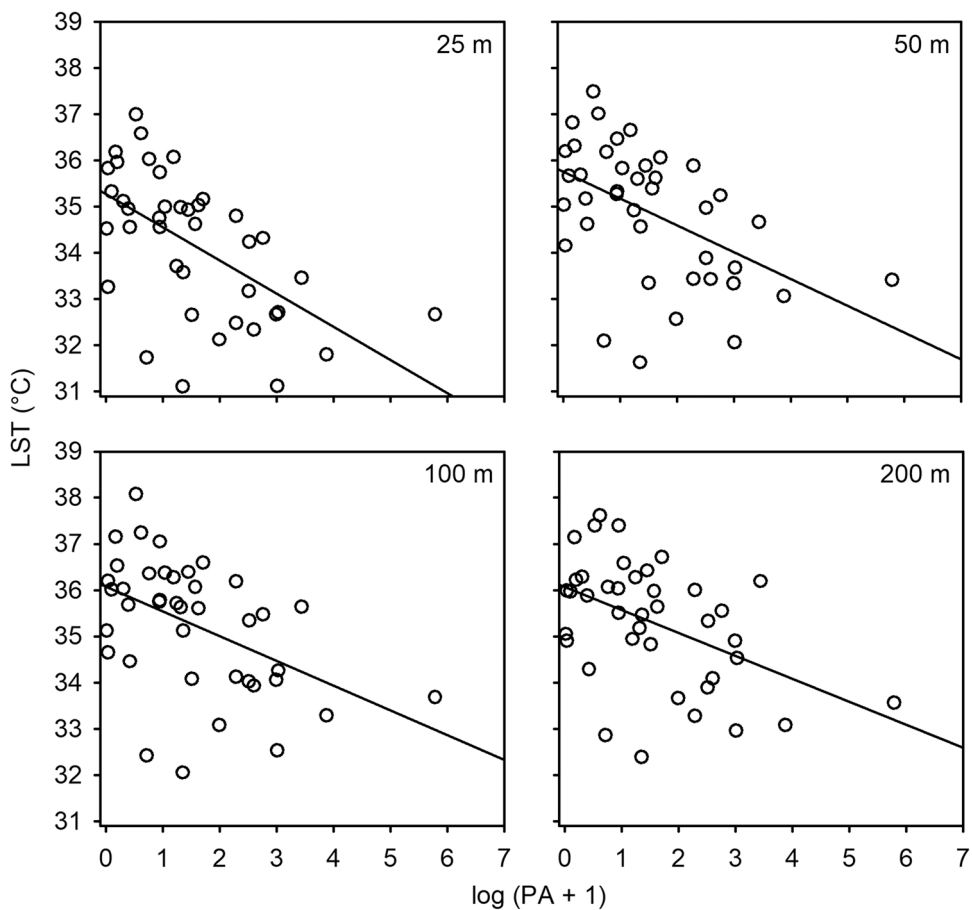


**Fig. 6.** Linear regression plots between mean LST and PA at different buffer distances.

not provide the same cooling effect (Duncan et al., 2019). Our results show that green spaces  $< 2$  ha exhibit LST  $2^{\circ}\text{C}$  higher than the mean value for all green patches  $> 1$  ha ( $33^{\circ}\text{C}$ ), and that areas  $\geq 6.4$  ha are necessary to decrease the LST by  $2^{\circ}\text{C}$  ( $31^{\circ}\text{C}$ ). Other research has found minimum size values of  $3.25$  ha (Kong et al., 2014) for green spaces to influence LST. There are reported saturation thresholds from which the decrease in LST is not influenced by larger patch size of the green spaces;  $40$  ha (Du et al., 2017),  $4.55$  ha (Yu et al., 2017),  $37$  ha (Huang et al., 2018). These methods are limited by the accuracy of the land cover classification, the minimum size and amount of urban green spaces considered, and the lack of other indicators which can be affecting the cooling capacity of the urban green infrastructure (e.g., tree species and their morphological and physiological characteristics).

Different and even contrasting findings between green spaces' overall shape and LST have been found. Our results show that the main overall shape of the green spaces of Xalapa is irregular, and that SI does not play a relevant role for LST nor cooling range in Xalapa. Most research studies have found that simple overall patch shapes (i.e., circle, square) are related to lower LST inside green spaces (Yu et al., 2017). Nevertheless, other evidence suggest the opposite relationship, in which a more irregular and even fragmented shape leads to lower LST (Chen et al., 2014; Du et al., 2017; Li et al., 2012). It has been found that patch shape affects cooling capacity especially in cold months (Chen et al., 2014). It would be necessary to explore the seasonal variation in Xalapa to determine if this is also true for this city. Nonetheless, the warmest time of the year is still the most relevant season to analyze SUHI, since it is when the urban inhabitants experience the strongest thermal comfort issues.

While other research has found that, for green spaces  $> 14$  ha, size is the most relevant factor influencing cooling (Jaganmohan et al., 2016),

in our study, independently of size, PA was the only important variable for LST inside green spaces. For cooling range, PA was complemented by Tc starting at the  $50$  m buffer and Tc was the only relevant variable at  $100$  m and  $200$  m, with a negative relationship between cooling range and distance. Literature suggests different distance thresholds up to which cooling range is provided by green spaces;  $50$  m (Chen et al., 2014),  $120$  m (Huang et al., 2018), and  $180$  m (Yu et al., 2017), pointing out the need of city-specific detailed analyzes. Although some authors suggest that several small green patches provide more efficient cooling than a single large patch of the same size (Kong et al., 2014; Yu et al., 2017), others found the opposite results (Cao et al., 2010). While these contrasting findings can be due to other local factors such as vegetation species composition, climate, built-up structure, among others, it is a fact that, independently of urban areas' size, mixed land cover at fixed distances has the potential to maximize the cooling range, as our findings show. Green spaces' cool island can be extended if it connects with neighboring smaller patches (mixed land cover), enhancing the cumulative cooling effect inside cities (Kong et al., 2014).

Despite being a region with high demand for heat mitigation inside cities, information on the cooling capacity of green spaces in Latin America is still limited (Palme, 2021). Moreover, most research conducted in this region has focused on large cities (e.g., Sao Paulo, Mexico City, Buenos Aires, Rio de Janeiro, Lima, Bogota and Santiago; Inostroza, 2014; Lemoine-Rodríguez et al., 2022; Palme, 2021). Yet, studies conducted for Latin American cities have confirmed the cooling potential of urban vegetation on LST (Colunga et al., 2015; Duarte et al., 2015; Gioia et al., 2014; Gomez-Martinez et al., 2021; Inostroza, 2014). Nevertheless, the cumulative cooling contribution of urban green spaces and scattered vegetation has been poorly explored with empirical data, especially for medium size cities (Palme, 2021).

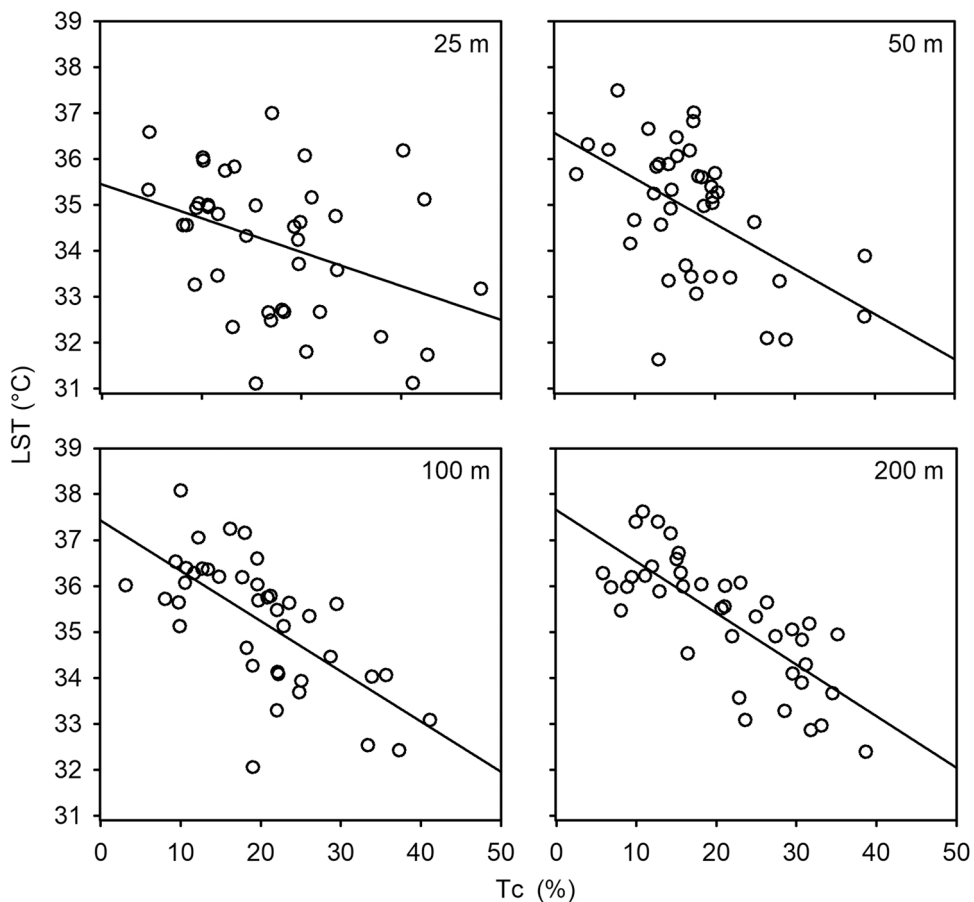


**Fig. 7.** Linear regression plots between mean LST and Tc at different buffer distances.

Limitations of this work should be considered when interpreting our results. We analyzed the cooling capacity of green spaces  $> 1$  ha composed by continuous tree cover, based on their size and shape. Therefore, smaller green patches were not assessed. Nevertheless, we included all tree cover patches when analyzing the effect of Tc at different distances from the green spaces  $> 1$  ha. We did not analyze the role of shrubs and grassland, which also contribute to cooling but in lower magnitude than trees (Kong et al., 2014). Other structural properties of green spaces that affect cooling, such as species composition, horizontal and vertical vegetation features, or green cover rate, were also out of our scope (Kong et al., 2014; Wang et al., 2021). Since we focused on green infrastructure, we did not analyze the spatial arrangement nor the composition of built-up and water bodies, which is important to include in further research to understand the thermal environment of Xalapa. While employing a recent image of the warmest month (i.e., April 2019) enabled us to understand the current state of the cooling capacity of urban green spaces in the most relevant time of the year for human thermal comfort, ad-hoc time-series analyzes are needed to understand the spatial and temporal LST trends of Xalapa.

#### 4.3. Implications for urban planning

Urban green infrastructure provides benefits to the urban ecosystem, such as recreation, flood retention, groundwater recharge, biodiversity, air filtering, carbon sequestration, and climate regulation (Burkhard et al., 2012; Chang et al., 2017; European Commission, 2014, 2013). Due to the challenges posed by climate change under the current, fast urbanizing scenario, the role of green spaces to mitigate heat has gained relevance for urban planning. In the case of Xalapa, our findings indicate that, to maximize their cooling capacity, green spaces should have a

minimum size of 2.8 ha and be complemented with other green patches beyond, at least 50 m (mixed land cover), to reach a cumulative cooling effect. This arrangement should be weighted with an urban agenda that limits urban sprawl towards a more compact green urban expansion (i.e., a less dispersed urban development that preserves greenspaces) than the one the city experienced in the past decades in order to define coherent planning paths (Lemoine-Rodríguez et al., 2019). Although other strategies have demonstrated relevance for heat mitigation, such as the implementation of low thermal building materials and modification of street canyons, vegetation is a less costly method to modify features for SUHI mitigation (Clinton and Gong, 2013). It is necessary to understand the local city-specific cooling capacity of green spaces in order to incorporate such information in urban planning agendas (Kong et al., 2014). Cooling capacity can be improved by maintaining a PA between the local optimal thresholds (Du et al., 2017) and implementing mixed land cover at fixed distances, thus maximizing the provision of climate regulation. Moreover, including high tree species diversity with dense tree cover in urban green spaces can further enhance their cooling capacity (Wang et al., 2021). Towards a climate adaptation approach, green infrastructure should be analyzed, planned, and administrated according to their spatial continuity and not following the administrative park limits, implying different types of management for single tree patches that provide cooling as one entity.

Further research analyzing the relationship between LST, the presence and structure of green spaces and socioeconomic level of the population can help identify city areas with high need of heat mitigation intervention (Duncan et al., 2019). For Xalapa, it has been found that public urban green spaces show a clustered pattern, with no presence of these spaces in almost half of its neighborhoods, and that the lower number, surface, and percent of greens spaces were associated with

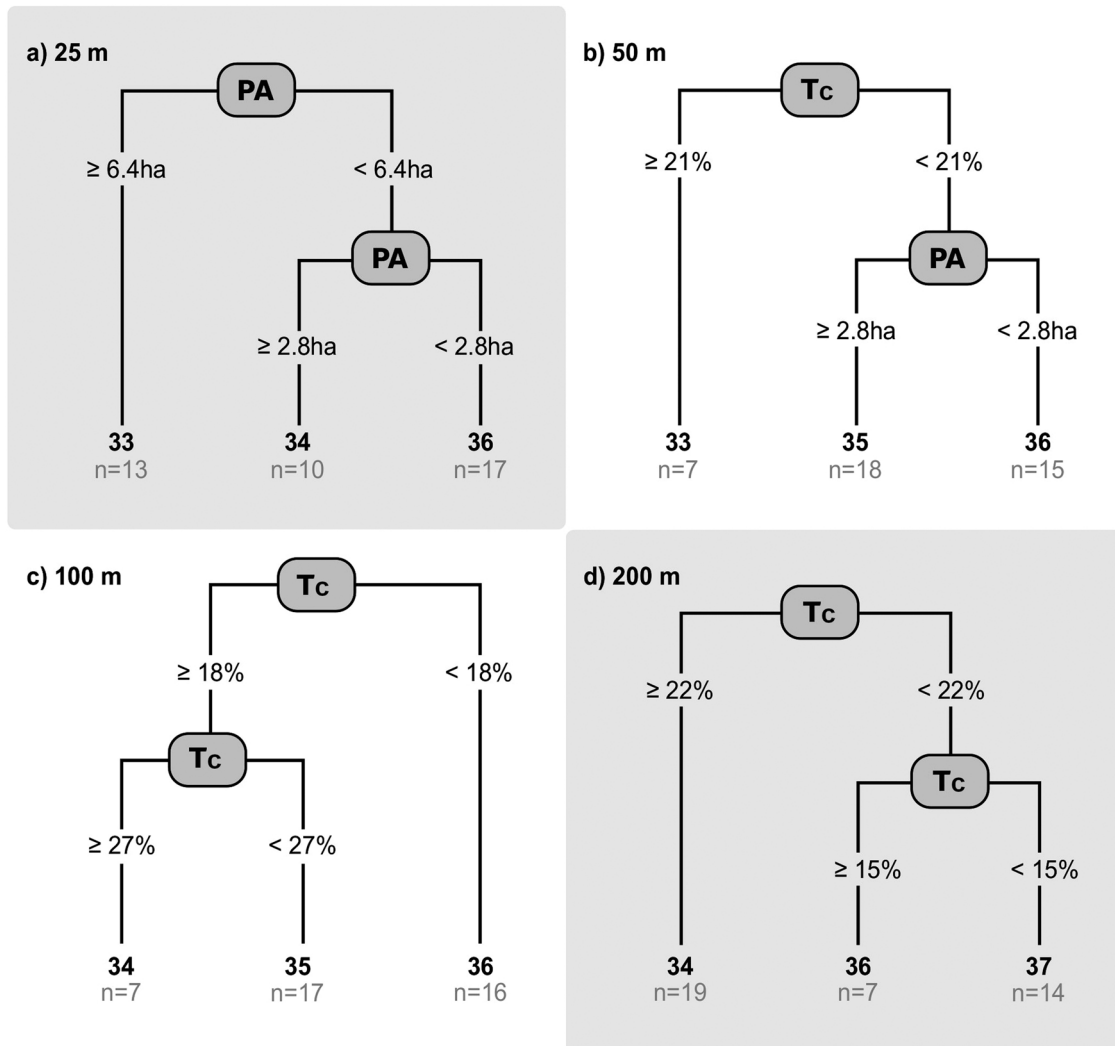


**Fig. 8.** Classification and regression trees (CARTs) showing the relationships between LST, PA, and Tc at different buffer distances.

areas of low socioeconomic level (Carmona-Ortega, 2021). Woefully, this is a common scenario in Mexican (Reyes-Plata and Gabriel-Bolea, 2018; Romo-Aguilar and de, 2008) and other Latin American cities (Gómez and Velázquez, 2018; Inostroza et al., 2016; Reyes-Päcke and Figueroa-Aldunce, 2010).

Moreover, empirical results are particularly important to understand the dynamics of SUHI in cities located in warm-humid climates, in which a strong increase on heat stress is projected due to the combination of high temperatures and air humidity (Zhao et al., 2014). Under the current climate change scenario, heat mitigation measures should be based on spatially explicit empirical data to properly inform planners. This information needs to be periodically updated and monitored to detect spatio-temporal trends and adapt the ongoing process of urban spatial planning.

## 5. Conclusions

In this study we analyzed the SUHI intensity of Xalapa during the warmest month (i.e., April) of 2019 and the cooling capacity of its urban green spaces  $> 1$  ha. Our results show that a green Neotropical city like Xalapa can exhibit a SUHI intensity of almost  $5^{\circ}\text{C}$ , with a mean urban LST of  $34.12^{\circ}\text{C}$ . The relationship between size of urban green spaces and Tc along the city with cooling range, outlines the need of green spaces with a minimum area of 2 ha to mitigate heat at  $\sim 2^{\circ}\text{C}$ . The size threshold of urban green spaces should be complemented with the

presence of scattered Tc starting at least 50 m from their borders (mixed land cover) to maximize the cooling capacity provided by the green infrastructure. At 50 m distance, areas with  $> 21\%$  of Tc exhibited the lowest LST ( $33^{\circ}\text{C}$ ), followed by zones with  $< 21\%$  of scattered Tc combined with parks  $\geq 2.8$  ha ( $35^{\circ}\text{C}$ ), which were  $1^{\circ}\text{C}$  cooler than areas with  $< 21\%$  of Tc and smaller parks ( $36^{\circ}\text{C}$ ). At 100 m and 200 m distance from parks' borders it is necessary to focus on the scattered Tc to mitigate heat, since park size does not influence LST at these distances. The contribution of mixed land cover to mitigate heat must be weighted with proper development agendas towards a compact green future urbanization in order to find feasible planning paths to implement adequate urban climate adaptation strategies.

## CRediT authorship contribution statement

**Richard Lemoine-Rodríguez:** Conceptualization, Methodology, Software, Investigation, Formal analysis, Data Curation, Writing – original draft, Writing – review & editing, Visualization. **Luis Inostroza:** Writing – review & editing. **Ina Falfán:** Formal analysis, Writing – original draft, Writing – review & editing, Visualization. **Ian MacGregor-Fors:** Conceptualization, Formal analysis, Writing – review & editing, Visualization.

## Declaration of Competing Interest

The authors declare that they have no known competing financial interests or personal relationships that could have appeared to influence the work reported in this paper.

## Acknowledgements

Richard Lemoine-Rodríguez acknowledges the PhD scholarship and financial support provided by the Consejo Nacional de Ciencia y Tecnología (CONACyT 308198/471027) and the Deutscher Akademischer Austauschdienst (DAAD 91680266). We are most grateful with ELLA for her careful revision of the English grammar.

## References

- Akbari, H., Kolokotsa, D., 2016. Three decades of urban heat islands and mitigation technologies research. *Energy Build.* 133, 834–842. <https://doi.org/10.1016/j.enbuild.2016.09.067>.
- Aleksandrowicz, O., Vuckovic, M., Kiesel, K., Mahdavi, A., 2017. Current trends in urban heat island mitigation research: observations based on a comprehensive research repository. *Urban Clim.* 21, 1–26. <https://doi.org/10.1016/j.uclim.2017.04.002>.
- Aram, F., Higueras García, E., Solgi, E., Mansournia, S., 2019a. Urban green space cooling effect in cities. *Heliyon* 5, e01339. <https://doi.org/10.1016/j.heliyon.2019.e01339>.
- Aram, F., Solgi, E., Higueras García, E., Mosavi, A., Várkonyi-Kóczy, A. R., 2019b. The cooling effect of large-scale urban parks on surrounding area thermal comfort. *Energies* 12, 3904. <https://doi.org/10.3390/en12203904>.
- Barradas, V.L., 1987. Evidencia del efecto de "Isla Térmica" en Jalapa, Veracruz, México. *Geofísica* 26, 125–135.
- Bowler, D.E., Buyung-Ali, L., Knight, T.M., Pullin, A.S., 2010. Urban greening to cool towns and cities: a systematic review of the empirical evidence. *Landscape Urban Plan.* 97, 147–155. <https://doi.org/10.1016/j.landurbplan.2010.05.006>.
- Burkhard, B., Kroll, F., Nedkov, S., Müller, F., 2012. Mapping ecosystem service supply, demand and budgets. *Ecol. Indic.* 21, 17–29. <https://doi.org/10.1016/j.ecolind.2011.06.019>.
- Cao, X., Onishi, A., Chen, J., Imura, H., 2010. Quantifying the cool island intensity of urban parks using ASTER and IKONOS data. *Landscape Urban Plan.* 96, 224–231. <https://doi.org/10.1016/j.landurbplan.2010.03.008>.
- Capitanachi, M.C., Utrera, E., Smith, C.B., 2004. El bosque urbano de Xalapa, Veracruz. Instituto de Ecología, A.C., Universidad Veracruzana, Sistema de Investigación del Golfo de México (Conacyt), Xalapa, Veracruz, México.
- Carmona-Ortega, M., 2021. Distribución espacial y provisión de servicios ecosistémicos culturales de las áreas verdes urbanas en la ciudad de Xalapa (Bachelor). Universidad Veracruzana, Xalapa, México.
- Castillo-Campos, G., 1991. Vegetación y flora del municipio de Xalapa, Veracruz. Instituto de Ecología, A.C., MAB UNESCO, H. Ayuntamiento de Xalapa, Veracruz, Xalapa, Veracruz, México.
- Chakraborty, T., Lee, X., 2019. A simplified urban-extent algorithm to characterize surface urban heat islands on a global scale and examine vegetation control on their spatiotemporal variability. *Int. J. Appl. Earth Obs. Geoinf.* 74, 269–280. <https://doi.org/10.1016/j.jag.2018.09.015>.
- Chakraborty, T., Hsu, A., Manya, D., Sheriff, G., 2020. A spatially explicit surface urban heat island database for the United States: characterization, uncertainties, and possible applications. *ISPRS J. Photogramm. Remote Sens.* 168, 74–88. <https://doi.org/10.1016/j.isprsjprs.2020.07.021>.
- Chang, J., Qu, Z., Xu, R., Pan, K., Xu, B., Min, Y., Ren, Y., Yang, G., Ge, Y., 2017. Assessing the ecosystem services provided by urban green spaces along urban center-edge gradients. *Sci. Rep.* 7, 11226. <https://doi.org/10.1038/s41598-017-11559-5>.
- Chavez, P.S., 1996. Image-based atmospheric corrections - revisited and improved. *Photogramm. Eng. Remote Sens.* 62, 1025–1036.
- Chen, A., Yao, X.A., Sun, R., Chen, L., 2014. Effect of urban green patterns on surface urban cool islands and its seasonal variations. *Urban For. Urban Green.* 13, 646–654. <https://doi.org/10.1016/j.ufug.2014.07.006>.
- Chibuike, E.M., Ibukun, A.O., Abbas, A., Kundu, J.J., 2018. Assessment of green parks cooling effect on Abuja urban microclimate using geospatial techniques. *Remote Sens. Appl. Soc. Environ.* 11, 11–21. <https://doi.org/10.1016/j.rsase.2018.04.006>.
- Clinton, N., Gong, P., 2013. MODIS detected surface urban heat islands and sinks: Global locations and controls. *Remote Sens. Environ.* 134, 294–304. <https://doi.org/10.1016/j.rse.2013.03.008>.
- Colunga, M.L., Cabromón-Sandoval, V.H., Suzán-Azpiri, H., Guevara-Escobar, A., Luna-Soria, H., 2015. The role of urban vegetation in temperature and heat island effects in Querétaro city. *Mex. Atmosfera* 28, 205–218.
- Du, H., Cai, W., Xu, Y., Wang, Z., Wang, Y., Cai, Y., 2017. Quantifying the cool island effects of urban green spaces using remote sensing data. *Urban For. Urban Green.* 27, 24–31. <https://doi.org/10.1016/j.ufug.2017.06.008>.
- Duarte, D.H.S., Shinzato, P., Gusson, C. dos, Alves, C.A., 2015. The impact of vegetation on urban microclimate to counterbalance built density in a subtropical changing climate. *Urban Clim.* 14, 224–239. <https://doi.org/10.1016/j.uclim.2015.09.006>.
- Duncan, J.M.A., Boruff, B., Saunders, A., Sun, Q., Hurley, J., Amati, M., 2019. Turning down the heat: an enhanced understanding of the relationship between urban vegetation and surface temperature at the city scale. *Sci. Total Environ.* 656, 118–128. <https://doi.org/10.1016/j.scitotenv.2018.11.223>.
- European Commission, 2013. Green Infrastructure (GI) — Enhancing Europe's Natural Capital (No. COM(2013) 249 final). European Commission, Brussels.
- European Commission, 2014. Building a green infrastructure for Europe. European Commission. Directorate General for the Environment, Belgium.
- Falfán, I., MacGregor-Fors, I., 2016. Woody neotropical streetscapes: a case study of tree and shrub species richness and composition in Xalapa. *Madera Bosques* 22, 95–110.
- Geng, X., Yu, Z., Zhang, D., Li, C., Yuan, Y., Wang, X., 2022. The influence of local background climate on the dominant factors and threshold-size of the cooling effect of urban parks. *Sci. Total Environ.* 823. <https://doi.org/10.1016/j.scitotenv.2022.153806>.
- Gioia, A., Paolini, L., Malizia, A., Oltra-Carrió, R., Sobrino, J.A., 2014. Size matters: vegetation patch size and surface temperature relationship in foothills cities of northwestern Argentina. *Urban Ecosyst.* 17, 1161–1174. <https://doi.org/10.1007/s11252-014-0372-1>.
- Gómez, N.J., Velázquez, G.A., 2018. Asociación entre los espacios verdes públicos y la calidad de vida en el municipio de Santa Fe, Argentina. *Cuad. Geogr. Rev. Colomb. Geogr.* 27, 164–179. <https://doi.org/10.15446/rdcg.v27n1.58740>.
- Gomez-Martinez, F., de Beurs, K.M., Koch, J., Widener, J., 2021. Multi-temporal land surface temperature and vegetation greenness in urban green spaces of Puebla, Mexico. *Land* 10, 155. <https://doi.org/10.3390/land10020155>.
- He, C., Zhou, L., Yao, Y., Ma, W., Kinney, P.L., 2021. Cooling effect of urban trees and its spatiotemporal characteristics: a comparative study. *Build. Environ.* 204. <https://doi.org/10.1016/j.buildenv.2021.108103>.
- Heisler, G.M., Brazel, A.J., 2010. The urban physical environment: temperature and urban heat islands. In: Aitkenhead-Peterson, J., Volder, A. (Eds.), *Urban Ecosystem Ecology, Agronomy Monograph 55*. American Society of Agronomy, Crop Science Society of America, Soil Science Society of America, Madison, Wisconsin, pp. 29–56.
- Higueras, E., 2006. Urbanismo bioclimático. GG, Barcelona.
- Huang, K., Li, X., Liu, X., Seto, K.C., 2019. Projecting global urban land expansion and heat island intensification through 2050. *Environ. Res. Lett.* 14, 114037. <https://doi.org/10.1088/1748-9326/ab4b71>.
- Huang, M., Cui, P., He, X., 2018. Study of the cooling effects of urban green space in Harbin in terms of reducing the heat island effect. *Sustainability* 10, 1101. <https://doi.org/10.3390/su10041101>.
- INEGI (Instituto Nacional de Estadística y Geografía), 2014. Anuario estadístico y geográfico de Veracruz de Ignacio de la Llave 2014. México.
- INEGI (Instituto Nacional de Estadística y Geografía), 2021. Censo de Población y Vivienda 2020. Microdatos para Veracruz de Ignacio de la Llave [WWW Document]. Inst. Nac. Estad. Geogr. URL <https://www.inegi.org.mx/programas/ccpv/2020/#Microdatos> (accessed 2.22.21).
- Inostroza, L., 2014. Open spaces and urban ecosystem services. Cooling effect towards urban planning in South American cities. *TEMA J. Land Use Mobil. Environ. Spec. Issue* 523–534. <https://doi.org/10.6092/1970-9870/2541>.
- Inostroza, L., Palme, M., de la Barrera, F., 2016. A heat vulnerability index: spatial patterns of exposure, sensitivity and adaptive capacity for Santiago de Chile. *PLoS One* 11, e0162464. <https://doi.org/10.1371/journal.pone.0162464>.
- Jaganmohan, M., Knapp, S., Buchmann, C.M., Schwarz, N., 2016. The bigger, the better? The influence of urban green space design on cooling effects for residential areas. *J. Environ. Qual.* 45, 134–145. <https://doi.org/10.2134/jeq2015.01.0062>.
- Kong, F., Yin, H., James, P., Hutyra, L.R., He, H.S., 2014. Effects of spatial pattern of greenspace on urban cooling in a large metropolitan area of eastern China. *Landscape Urban Plan.* 128, 35–47. <https://doi.org/10.1016/j.landurbplan.2014.04.018>.
- Kottek, M., Grieser, J., Beck, C., Rudolf, B., Rubel, F., 2006. World Map of the Köppen-Geiger climate classification updated. *Meteorol. Z.* 15, 259–263. <https://doi.org/10.1127/0941-2948/2006/0130>.
- Lai, D., Liu, W., Gan, T., Liu, K., Chen, Q., 2019. A review of mitigating strategies to improve the thermal environment and thermal comfort in urban outdoor spaces. *Sci. Total Environ.* 661, 337–353. <https://doi.org/10.1016/j.scitotenv.2019.01.062>.
- Lemoine-Rodríguez, R., Mas, J.-F., 2020. LSTtools: An R package to process thermal data derived from Landsat and MODIS images (v0.0.2). Zenodo <https://doi.org/10.5281/zenodo.4010732>.
- Lemoine-Rodríguez, R., MacGregor-Fors, I., Muñoz-Robles, C., 2019. Six decades of urban green change in a neotropical city: a case study of Xalapa, Veracruz, Mexico. *Urban Ecosyst.* 22, 609–618. <https://doi.org/10.1007/s11252-019-00839-9>.
- Lemoine-Rodríguez, R., Inostroza, L., Zepp, H., 2020. The global homogenization of urban form: An assessment of 194 cities across time. *Landscape Urban Plan.* 204, 103949. <https://doi.org/10.1016/j.landurbplan.2020.103949>.
- Lemoine-Rodríguez, R., Inostroza, L., Zepp, H., 2022. Intraurban heterogeneity of space-time land surface temperature trends in six climate-diverse cities. *Sci. Total Environ.* 804, 150037. <https://doi.org/10.1016/j.scitotenv.2021.150037>.
- Lenth, R., Singmann, H., Love, J., Buerkner, P., Herve, M., 2020. Package “emmeans”: Estimated marginal means, aka least-squares means. Package version 1.4.5. (<https://cran.r-project.org/web/packages/emmeans/emmeans.pdf>).
- Leutner, B., Horning, N., Schwalb-Willmann, J., Hijmans, R.J., 2019. RStoolbox: Tools for Remote Sensing Data Analysis (R package version 0.2.6) (<https://cran.r-project.org/web/packages/RStoolbox/RStoolbox.pdf>).
- Li, X., Zhou, W., Ouyang, Z., Xu, W., Zheng, H., 2012. Spatial pattern of greenspace affects land surface temperature: evidence from the heavily urbanized Beijing metropolitan area, China. *Landscape Ecol.* 27, 887–898. <https://doi.org/10.1007/s10980-012-9731-6>.
- Liang, Z., Wu, S., Wang, Y., Wei, F., Huang, J., Shen, J., Li, S., 2020. The relationship between urban form and heat island intensity along the urban development

- gradients. *Sci. Total Environ.* 708, 135011 <https://doi.org/10.1016/j.scitotenv.2019.135011>.
- Lin, W., Yu, T., Chang, X., Wu, W., Zhang, Y., 2015. Calculating cooling extents of green parks using remote sensing: method and test. *Landscape Urban Plan.* 134, 66–75. <https://doi.org/10.1016/j.landurbplan.2014.10.012>.
- Li, H., Huang, B., Zhan, Q., Gao, S., Li, R., Fan, Z., 2021. The influence of urban form on surface urban heat island and its planning implications: evidence from 1288 urban clusters in China. *Sustain. Cities Soc.* 71, 102987 <https://doi.org/10.1016/j.scs.2021.102987>.
- Lu, L., Weng, Q., Xiao, D., Guo, H., Li, Q., Hui, W., 2020. Spatiotemporal variation of surface urban heat islands in relation to land cover composition and configuration: A multi-scale case study of Xi'an, China. *Remote Sens.* 12, 2713. <https://doi.org/10.3390/rs12172713>.
- MacGregor-Fors, I., 2010. How to measure the urban-wildland ecotone: redefining ‘peri-urban’ areas. *Ecol. Res.* 25, 883–887. <https://doi.org/10.1007/s11284-010-0717-z>.
- Martilli, A., Krayenhoff, E.S., Nazarian, N., 2020. Is the Urban Heat Island intensity relevant for heat mitigation studies? *Urban Clim.* 31, 100541 <https://doi.org/10.1016/j.ulclim.2019.100541>.
- McGarigal, K., Cushman, S., Ene, E., 2012. FRAGSTATS v4: Spatial Pattern Analysis Program for Categorical and Continuous Maps. Computer software program produced by the authors at the University of Massachusetts, Amherst.
- Méndez Romero, E.A., 2017. Alteraciones térmicas derivadas de la urbanización en la ciudad de Xalapa, Veracruz. Análisis espacial y temporal: 1982–2015 (Master). El Colegio de Veracruz, Xalapa, México.
- Mohajerani, A., Bakaric, J., Jeffrey-Bailey, T., 2017. The urban heat island effect, its causes, and mitigation, with reference to the thermal properties of asphalt concrete. *J. Environ. Manag.* 197, 522–538. <https://doi.org/10.1016/j.jenvman.2017.03.095>.
- Montaner-Fernández, D., Morales-Salinas, L., Rodríguez, J.S., Cárdenas-Jirón, L., Huete, A., Fuentes-Jaque, G., Pérez-Martínez, W., Cabezas, J., 2020. Spatio-temporal variation of the urban heat island in Santiago, Chile during summers 2005–2017. *Remote Sens.* 12, 3345. <https://doi.org/10.3390/rs12203345>.
- Monteiro, F.F., Gonçalves, W.A., Andrade, L., de, M.B., Villavicencio, L.M.M., Silva, C.M., dos, S., 2021. Assessment of Urban Heat Islands in Brazil based on MODIS remote sensing data. *Urban Clim.* 35, 100726 <https://doi.org/10.1016/j.ulclim.2020.100726>.
- Nichol, J.E., Fung, W.Y., Lam, K.-S., Wong, M.S., 2009. Urban heat island diagnosis using ASTER satellite images and ‘in situ’ air temperature. *Atmos. Res.* 94, 276–284. <https://doi.org/10.1016/j.atmosres.2009.06.011>.
- Norton, B.A., Coutts, A.M., Livesley, S.J., Harris, R.J., Hunter, A.M., Williams, N.S.G., 2015. Planning for cooler cities: a framework to prioritise green infrastructure to mitigate high temperatures in urban landscapes. *Landscape Urban Plan.* 134, 127–138. <https://doi.org/10.1016/j.landurbplan.2014.10.018>.
- Nuruzzaman, Md, 2015. Urban heat island: Causes, effects and mitigation measures - a review. *Int. J. Environ. Monit. Anal.* 3, 67. <https://doi.org/10.11648/j.ijema.20150302.15>.
- Oke, T.R., 1973. City size and the urban heat island. *Atmos. Environ.* 7, 769–779.
- Oke, T.R., 1995. The heat island of the urban boundary layer: characteristics, causes and effects. In: Cermak, J.E., Davenport, A.G., Plate, E.J., Viegas, D.X. (Eds.), *Wind Climate in Cities*. Springer, Netherlands, Dordrecht, pp. 81–107. [https://doi.org/10.1007/978-94-017-3686-2\\_5](https://doi.org/10.1007/978-94-017-3686-2_5).
- Oke, T.R., Mills, G., Christen, A., Voogt, J.A., 2017. *Urban climates*. Cambridge University Press, Cambridge.
- Palme, M., 2021. Urban heat island studies in hot and humid climates: a review of the state of art in Latin-America. In: Enteria, N., Santamouris, M., Eicker, U. (Eds.), *Urban Heat Island (UHI) Mitigation: Hot and Humid Regions, Advances in 21st Century Human Settlements*. Springer, Singapore, pp. 123–141. [https://doi.org/10.1007/978-981-33-4050-3\\_6](https://doi.org/10.1007/978-981-33-4050-3_6).
- Peng, S., Piao, S., Ciais, P., Friedlingstein, P., Ottle, C., Bréon, F.-M., Nan, H., Zhou, L., Myreni, R.B., 2012. Surface urban heat island across 419 global big cities. *Environ. Sci. Technol.* 46, 696–703. <https://doi.org/10.1021/es2030438>.
- Pereyra Díaz, D., Palma Grayeb, B.E., Zitacuaro, C.I., 1992. Correlation between northers of Gulf of Mexico and frosts at Las Vigas, Veracruz, Mexico. *Atmósfera* 5, 109–118.
- Pinheiro, J., Bates, D., DebRoy, S., Sarkar, D., 2020. Package nlme: linear and nonlinear mixed effects models. R. Package Version 3, 1–145. (<https://cran.r-project.org/web/packages/nlme/nlme.pdf>).
- Prihodko, L., Goward, S.N., 1997. Estimation of air temperature from remotely sensed surface observations. *Remote Sens. Environ.* 60, 335–346. [https://doi.org/10.1016/S0034-4257\(96\)00216-7](https://doi.org/10.1016/S0034-4257(96)00216-7).
- R Core Team, 2019. R: A language and environment for statistical computing. R Foundation for Statistical Computing, Vienna, Austria.
- Reyes-Pácke, S., Figueroa-Alduña, I.M., 2010. Distribución, superficie y accesibilidad de las áreas verdes en Santiago de Chile. *EURE* 36, 89–110. <https://doi.org/10.4067/S0250-7161201000030004>.
- Reyes-Plata, J., Gabriel-Bolea, C., 2018. Distribución de las áreas verdes, índice de marginación y justicia ambiental en León, Guanajuato. In: Pérez Campuzano, E., Mota-Flores, V.E. (Eds.), *Desarrollo Regional Sustentable y Turismo*. Universidad Nacional Autónoma de México. Asociación Mexicana de Ciencias para el Desarrollo Regional A.C., México, pp. 176–203.
- Rizwan, A.M., Dennis, L.Y.C., Liu, C., 2008. A review on the generation, determination and mitigation of urban heat island. *J. Environ. Sci.* 20, 120–128. [https://doi.org/10.1016/S1001-0742\(08\)60019-4](https://doi.org/10.1016/S1001-0742(08)60019-4).
- Romo-Aguilar, M., de, L., 2008. Áreas verdes y justicia social en Ciudad Juárez, Chihuahua. *Crisol* 3, 9–26.
- Roth, M., 2007. Review of urban climate research in (sub)tropical regions. *Int. J. Climatol.* 27, 1859–1873. <https://doi.org/10.1002/joc.1591>.
- Rzedowski, J., 1978. Vegetación de México. Limusa, México, D.F.
- Santamouris, M., 2015. Analyzing the heat island magnitude and characteristics in one hundred Asian and Australian cities and regions. *Sci. Total Environ.* 512–513, 582–598. <https://doi.org/10.1016/j.scitotenv.2015.01.060>.
- Sarricolea, P., Meseguer-Ruiz, O., 2019. Urban climates of large cities: comparison of the urban heat island effect in Latin America. In: Henríquez, C., Romero, H. (Eds.), *Urban Climates in Latin America*. Springer International Publishing, Cham, pp. 17–32. [https://doi.org/10.1007/978-3-319-97013-4\\_2](https://doi.org/10.1007/978-3-319-97013-4_2).
- Schwarz, N., Manceur, A.M., 2015. Analyzing the influence of urban forms on surface urban heat islands in Europe. *J. Urban Plan. Dev.* 141, A4014003 [https://doi.org/10.1061/\(ASCE\)UP.1943-5444.0000263](https://doi.org/10.1061/(ASCE)UP.1943-5444.0000263).
- Sobrino, J.A., Jiménez-Muñoz, J.C., Soria, G., Romaguera, M., Guanter, L., Moreno, J., Plaza, A., Martínez, P., 2008. Land surface emissivity retrieval from different VNIR and TIR sensors. *IEEE Trans. Geosci. Remote Sens.* 46, 316–327.
- Soto-Esparragoza, M., Gómez-Columna, M., 1993. Consideraciones climáticas de la ciudad de Xalapa, in: López-Moreno, I.R. (Ed.), *Ecología Urbana Aplicada a La Ciudad de Xalapa*. Instituto de Ecología, A.C., MAB UNESCO, H. Ayuntamiento de Xalapa, Veracruz, Xalapa, Veracruz, México, pp. 81–98.
- Stone, B., Hess, J.J., Frumkin, H., 2010. Urban form and extreme heat events: are sprawling cities more vulnerable to climate change than compact cities? *Environ. Health Perspect.* 118, 1425–1428. <https://doi.org/10.1289/ehp.901879>.
- Tan, J., Zheng, Y., Tang, X., Guo, C., Li, L., Song, G., Zhen, X., Yuan, D., Kalkstein, A.J., Li, F., Chen, H., 2010. The urban heat island and its impact on heat waves and human health in Shanghai. *Int. J. Biometeorol.* 54, 75–84. <https://doi.org/10.1007/s00484-009-0256-x>.
- Tejeda-Martínez, A., Acevedo-Rosas, F., 1990. Alteraciones climáticas por la urbanización en Xalapa. *Ver. Cienc. El Hombre* 6, 37–48.
- Therneau, T., Atkinson, B., 2018. Package “rpart”: Recursive Partitioning and Regression Trees. R. Package Version 4, 1–13. (<https://CRAN.R-project.org/package=rpart>).
- United Nations, Department of Economic and Social Affairs, Population Division, 2019. *World Urbanization Prospects: The 2018 Revision* (No. ST/ESA/SER.A/420). United Nations, New York.
- USGS (United States Geological Service), 2019. Landsat 8 data users handbook. USGS Earth Resources Observation and Science, Sioux Falls, South Dakota, USA.
- Voogt, J.A., Oke, T.R., 2003. Thermal remote sensing of urban climates. *Remote Sens. Environ.* 86, 370–384. [https://doi.org/10.1016/S0034-4257\(03\)00079-8](https://doi.org/10.1016/S0034-4257(03)00079-8).
- Wang, X., Dallimer, M., Scott, C.E., Shi, W., Gao, J., 2021. Tree species richness and diversity predicts the magnitude of urban heat island mitigation effects of greenspaces. *Sci. Total Environ.* 770, 145211 <https://doi.org/10.1016/j.scitotenv.2021.145211>.
- Weng, Q., Lu, D., Schubring, J., 2004. Estimation of land surface temperature–vegetation abundance relationship for urban heat island studies. *Remote Sens. Environ.* 89, 467–483. <https://doi.org/10.1016/j.rse.2003.11.005>.
- Xiao, X.D., Dong, L., Yan, H., Yang, N., Xiong, Y., 2018. The influence of the spatial characteristics of urban green space on the urban heat island effect in Suzhou Industrial Park. *Sustain. Cities Soc.* 40, 428–439. <https://doi.org/10.1016/j.scs.2018.04.002>.
- Xu, X., Sun, S., Liu, W., García, E.H., He, L., Cai, Q., Xu, S., Wang, J., Zhu, J., 2017. The cooling and energy saving effect of landscape design parameters of urban park in summer: a case of Beijing, China. *Energy Build.* 149, 91–100. <https://doi.org/10.1016/j.enbuild.2017.05.052>.
- Xu, X., Liu, S., Sun, S., Zhang, W., Liu, Y., Lao, Z., Guo, G., Smith, K., Cui, Y., Liu, W., Higueras García, E., Zhu, J., 2019. Evaluation of energy saving potential of an urban green space and its water bodies. *Energy Build.* 188–189, 58–70. <https://doi.org/10.1016/j.enbuild.2019.02.003>.
- Yan, H., Wu, F., Dong, L., 2018. Influence of a large urban park on the local urban thermal environment. *Sci. Total Environ.* 622–623, 882–891. <https://doi.org/10.1016/j.scitotenv.2017.11.327>.
- Yang, P., Xiao, Z.-N., Ye, M.-S., 2016. Cooling effect of urban parks and their relationship with urban heat islands. *Atmos. Ocean. Sci. Lett.* 9, 298–305. <https://doi.org/10.1080/16742834.2016.1191316>.
- Yang, Q., Huang, X., Yang, J., Liu, Y., 2021. The relationship between land surface temperature and artificial impervious surface fraction in 682 global cities: spatiotemporal variations and drivers. *Environ. Res. Lett.* 16, 024032 <https://doi.org/10.1088/1748-9326/abdaed>.
- Yow, D.M., 2007. Urban heat islands: Observations, impacts, and adaptation. *Geogr. Compass* 1, 1227–1251. <https://doi.org/10.1111/j.1749-8198.2007.00063.x>.
- Yu, Z., Guo, X., Jørgensen, G., Vejre, H., 2017. How can urban green spaces be planned for climate adaptation in subtropical cities? *Ecol. Indic.* 82, 152–162. <https://doi.org/10.1016/j.ecolind.2017.07.002>.
- Zhao, L., Lee, X., Smith, R.B., Oleson, K., 2014. Strong contributions of local background climate to urban heat islands. *Nature* 511, 216–219. <https://doi.org/10.1038/nature13462>.
- Zhao, L., Oppenheimer, M., Zhu, Q., Baldwin, J.W., Ebi, K.L., Bou-Zeid, E., Guan, K., Liu, X., 2018. Interactions between urban heat islands and heat waves. *Environ. Res. Lett.* 13, 034003 <https://doi.org/10.1088/1748-9326/aa9f73>.